METHODS FOR THE DETERMINATION OF Z AND M USING dE/dx, ČERENKOV, AND TOTAL ENERGY MEASUREMENTS*

E. C. Stone

California Institute of Technology
Pasadena, California 91125

*Invited paper presented at the ESRO workshop on "Research Goals for Cosmic Ray Astrophysics in the 1980's", Frascati, Italy, 24, 25 October 1974.

October 1974
SRL 74-4

FIGURE CAPTIONS AND COMMENTS

FIGURE 1 This figure provides a schematic (and simplified) illustration of the determination of the mass M of a cosmic ray nuclide with charge Z and kinetic energy E by using the dE/dx-E technique. The particle penetrates a detector of thickness L, depositing ionization energy ΔE in that detector and depositing its residual energy E' in a second detector. For the purposes of an illustrative calculation, it is assumed that the range R of a particle with total kinetic energy E (where $E = E' + \Delta E$) is given by a power law expression. A similar expression is assumed for a particle of range R-L and energy E'.

As shown, the two expressions can be solved for M. The expression for M emphasizes the point that any uncertainities in ΔE (such as Landau fluctuations), E' (such as scintillator irregularities), L (such as unknown incidence angles), or in any of the other parameters will result in an uncertainty in the derived value for M.

FIGURE 2 This figure illustrates the dE/dx-E mass identification technique. The events shown are a small sample of $\sim 10^6$ events accumulated during the calibration of the Caltech Electron/Isotope Spectrometer which is currently operational on the IMP-7 and IMP-8 spacecraft. In this case, ΔE was measured in a 50μm thick silicon surface barrier detector and E' was measured in a 1mm thick silicon detector. Tracks corresponding to ^{6}Li, ^{7}Li, ^{8}Li, ^{7}Be, ^{9}Be, ^{10}Be, ^{10}B, ^{11}B, and ^{12}B are evident. The mass resolution, which is dominated in this case by thickness non-uniformities in the 50μm

detector, is $\sigma_m \approx 0.2$ amu. The calibration was done on the 88" cyclotron at the Lawrence Berkeley Laboratory.

FIGURE 3 This plot summarizes typical mass resolutions reported for various recent satellite experiments using the dE/dx-E technique for the isotopes of elements up through Z = 8. On the right there are four lines labelled 1:1, 2:1, 10:1, and 100:1 which are intended to indicate the mass resolution required to resolve adjacent isotopes with the specified relative abundances.

Also shown are typical mass resolutions which analysis indicates can be expected for different versions of the dE/dx-E technique. The resolution of the disk detector systems is limited primarily by variations in the path-length L. These systems will be able to resolve isotopes with $Z \leqslant 8$. The Chicago group pioneered the use of curved ΔE detectors in order to reduce the uncertainty in L. The use of multiple ΔE measurements will further improve resolution of the curved detector system, permitting the resolution of adjacent isotopes up to $Z \approx 14$. Finally, the use of position sensing should provide isotopic resolution up through $Z \approx 28$.

FIGURE 4 This figure provides a schematic (and simplified) illustration of the $\check{C}$ x E method of mass determination. A cosmic ray nuclide (total kinetic energy E, mass M, charge Z, velocity βc) penetrates a Čerenkov radiator (thickness L, refractive index N) and stops in a detector which measures the energy E. For illustration, the ΔE in the Čerenkov radiator is neglected. The expression for the Čerenkov signal $\check{C}$ and the kinetic

energy signal E are shown, where $\gamma = (1-\beta^2)^{-1/2}$. These two expressions can be solved for M as shown. The expression for M emphasizes that any uncertainty in E (such as due to scintillator resolution), C (photo-electron statistics), K (variations in $\check{C}$ light collection), and L will result in an uncertainty in M.

FIGURE 5 This figure includes an analysis of the expected mass resolution for ^{56}Fe. The upper solid curve corresponds to what is probably possible with the current techniques. For comparison, the mass resolution obtained by the University of New Hampshire group several years ago is shown. Adjacent isotopes of Fe will not be resolved unless significant improvements are made. To indicate what might be possible, the lower solid curve shows the expected resolution if the uncertainty in the pathlength L and in the energy E could both be improved approximately an order of magnitude. Note that in this case, σ_m would be less than 0.2 amu for an energy interval of ~ 50 MeV/nuc above the $\check{C}$ threshold. The low energy limit of the curves has been set by an assumed scintillation efficiency of the $\check{C}$ radiator corresponding to 5% of the $\check{C}$ signal for $\beta = 1$.

The dashed lines indicate the fraction of Fe events which do not suffer inelastic nuclear collision in the process of stopping in the E detector. Approximately 50%, 30% and 20% of the 400 MeV/nuc nuclei would interact in plastic, Si, and CsI detectors, resulting not only in a reduced detection efficiency, but producing presently unknown background effects. The evaluation of such systematic background effects will require careful calibration. Those events (~ 1%) suffering single neutron stripping may be particularly troublesome.

FIGURE 6 This figure provides a summary of typical mass resolutions reported at $\geq$ 100 MeV/nuc by a number of groups using a variety of stopping-particle techniques. Except for the Kiel results which were obtained during an accelerator calibration, all of these results were obtained with balloon instruments. The upper dashed line indicates the expected mass resolution for the $\check{C}$ x E technique with current technology, while the lower dashed curve indicates what might be possible if the measurement of L and E could be improved an order of magnitude. Also shown is the expected resolution of the Berkeley multi-element silicon detector telescope which will be on ISEE (Heliocentric).

FIGURE 7 This figure is a table of typical future satellite experiments employing the dE/dx-E technique. The table is not intended as a complete list of confirmed experiments, especially in the case of European experiments and missions. The numbers in the table are my estimates of the instrument characteristics and have not been verified with the various investigators. Note that disk detector systems should be able to resolve adjacent isotopes up to $Z \leq 8$, curved detector systems with multi-parameter analysis up to $Z \leq 14$, and position sensing systems up to $Z \leq 28$.

FIGURE 8 This figure shows what might be expected for the fluxes of isotopes of each element in the ~ 100 to ~ 400 MeV/nuc interval at solar minimum. The relative abundances were obtained from Tsao, Shapiro, and Silberberg (Denver Conference). Each nuclide in their Table 1 is plotted.

The dashed points correspond to the survival of $^{26}A\ell$ and ^{36}Cl.

Also shown are the minimum flux levels required to obtain 10 events of each nuclide for 3 typical examples (ignoring nuclear interaction effects). The upper dashed line corresponds to an instrument similar to the ISEE (Heliocentric) GSFC experiment with an energy interval of 100 MeV/nuc. The lower dashed line corresponds both to a balloon instrument, similar to the UNH $\check{C}$ x E experiment, and to a satellite experiment similar to the Berkeley instrument on ISEE (Heliocentric).. The latter line has been adjusted upward to compensate for the reduced fluxes at solar maximum.

FIGURE 9 This figure shows the charge distribution obtained with the Washington University $1m^2$ dE/dx-$\check{C}$ telescope in 1970. In this pioneering experiment, the charge resolution was $\sigma_z \sim 0.63$, permitting the resolution of even - Z nuclei with relative abundances of 3 or 4 to 1. Odd - Z nuclei were not resolved.

FIGURE 10 This figure shows the charge distribution obtained by Washington University in 1972 when the second generation HEAO design concepts and other modifications were included in the balloon instrument. The charge resolution was $\sigma_z \sim 0.33$, permitting the resolution of both even and odd - Z nuclei with relative abundances of 2 or 3 to 1 for adjacent elements.

FIGURE 11 This figure summarizes the resolution obtained for Fe with the balloon instrument and indicates the further improvement which should be possible with the actual HEAO-C instrument. The solid curve indicates on the vertical axis the maximum resolvable abundance ratio for adjacent

elements as a function of the charge resolution. The dashed curve indicates the same information for adjacent even - Z nuclei.

FIGURE 12 This figure tabulates some of the characteristics of the two presently planned UH cosmic ray satellite experiments. The UK-6 instrument is an extremely light weight instrument with rather large collecting power because of the spherical geometry. The dE/dx signal is measured in a spherical gas scintillation detector and the $\check{C}$ signal in a spherical shell of Pilot 425. The instrument is carefully designed so that hodoscope information is unnecessary.

The HEAO-C experiment is a larger instrument of more conventional planar geometry. The dE/dx signal is measured in parallel plate pulse ionization chambers and the $\check{C}$ signal in a planar Lucite radiator. A multiwire ionization hodoscope provides the directional information.

dE/dX — E TECHNIQUE

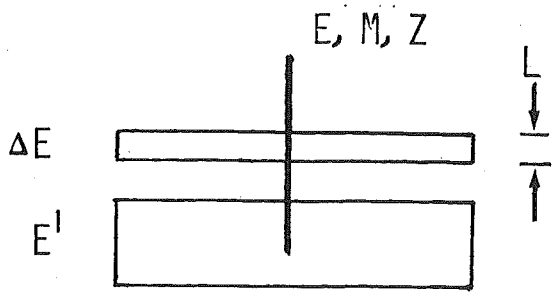

ILLUSTRATIVE CALCULATION

$$R = \frac{KM}{Z^2}\left(\frac{E' + \Delta E}{M}\right)^a$$

$$R - L = \frac{KM}{Z^2}\left(\frac{E'}{M}\right)^a$$

SOLVE FOR M

$$M = \left(\frac{K}{LZ^2}\right)^{\frac{1}{a-1}}\left[(E' + \Delta E)^a - E'^a\right]^{\frac{1}{a-1}}$$

Fig.1

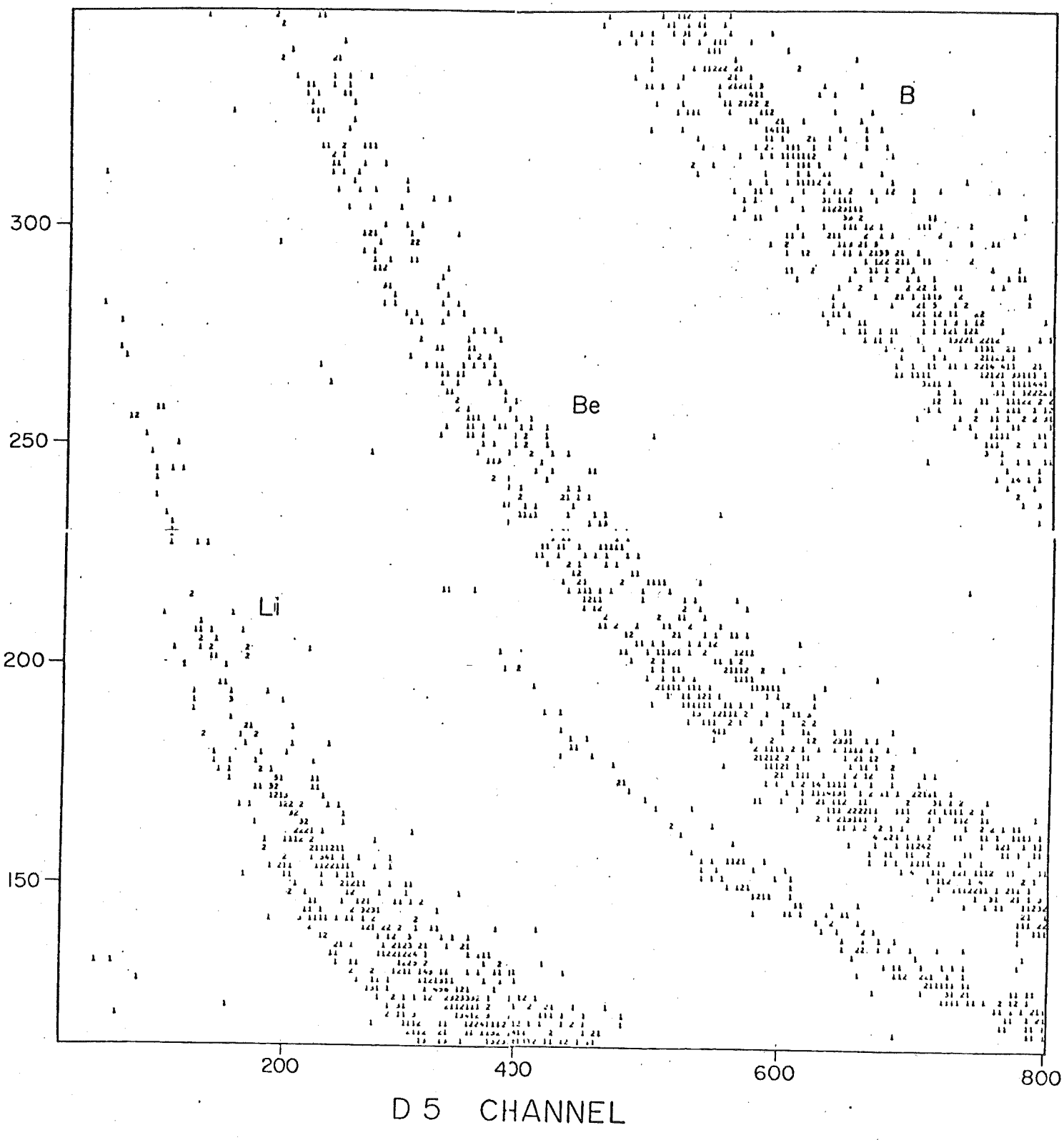

Fig. 2

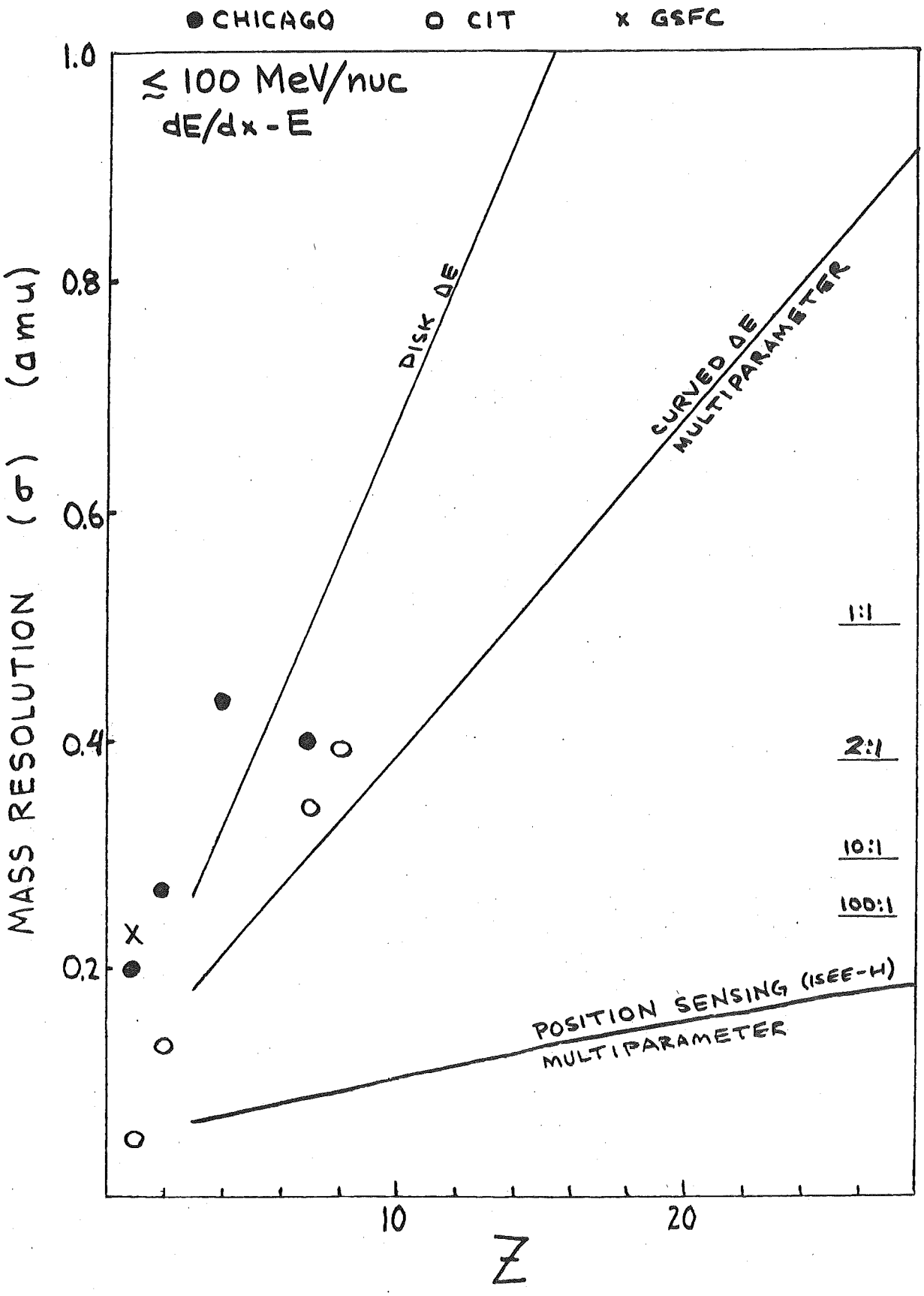
● CHICAGO
○ CIT
x GSFC
≲ 100 MeV/nuc
dE/dx - E
DISK ΔE
CURVED ΔE
MULTIPARAMETER
1:1
2:1
10:1
100:1
POSITION SENSING (ISEE-H)
MULTIPARAMETER
MASS RESOLUTION (σ) (amu)
1.0
0.8
0.6
0.4
0.2
10
20
Z

Fig. 3

$\check{C}$ x E TECHNIQUE

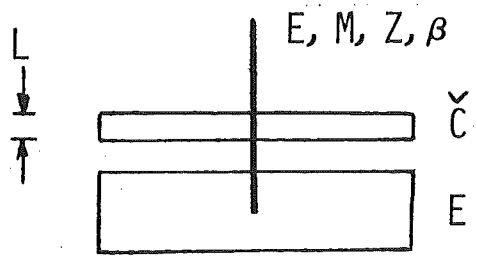

ILLUSTRATIVE CALCULATION

(NEGLECT ΔE IN L)

$$\check{C} = KLZ^2 \left(1 - \beta_t^2/\beta^2\right)$$

$$E = (\gamma - 1)\ Mc^2$$

WHERE

$$\beta_t = 1/N$$

SOLVE FOR M

$$M = \frac{E}{\left[\left\{\frac{1 - \check{C}/KLZ^2}{1 - \check{C}/KLZ^2 - \beta_t^2}\right\}^{1/2} - 1\right] c^2}$$

Fig. 4

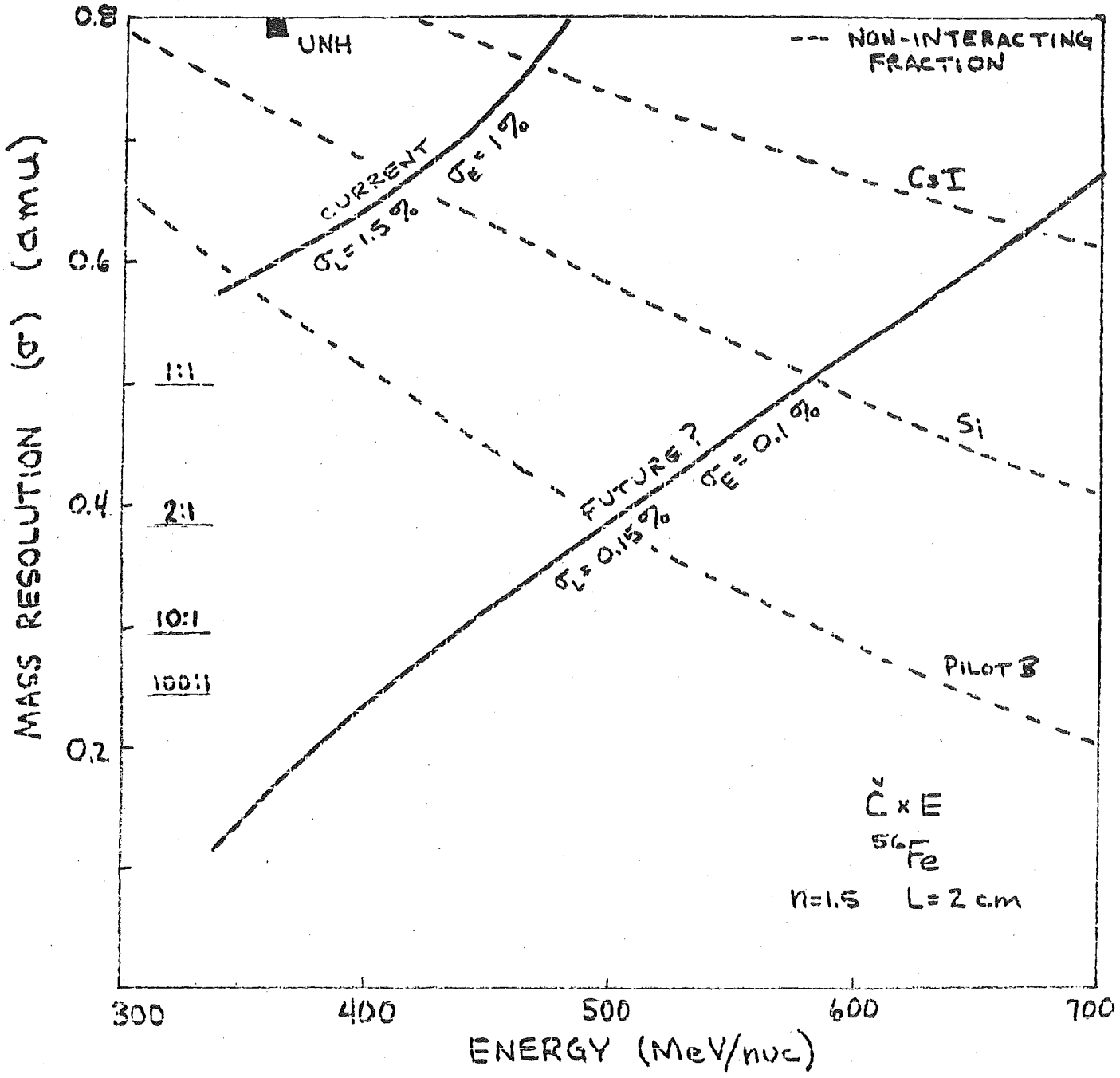
0.8
0.6
0.4
0.2
MASS RESOLUTION (σ) (amu)
UNH
--- NON-INTERACTING FRACTION
CURRENT
σE = 1%
σL = 1.5%
CsI
Si
PILOT B
FUTURE?
σE = 0.1%
σL = 0.15%
1:1
2:1
10:1
100:1
Č x E
56Fe
n=1.5 L=2 cm
300
400
500
600
700
ENERGY (MeV/nuc)

Fig. 5

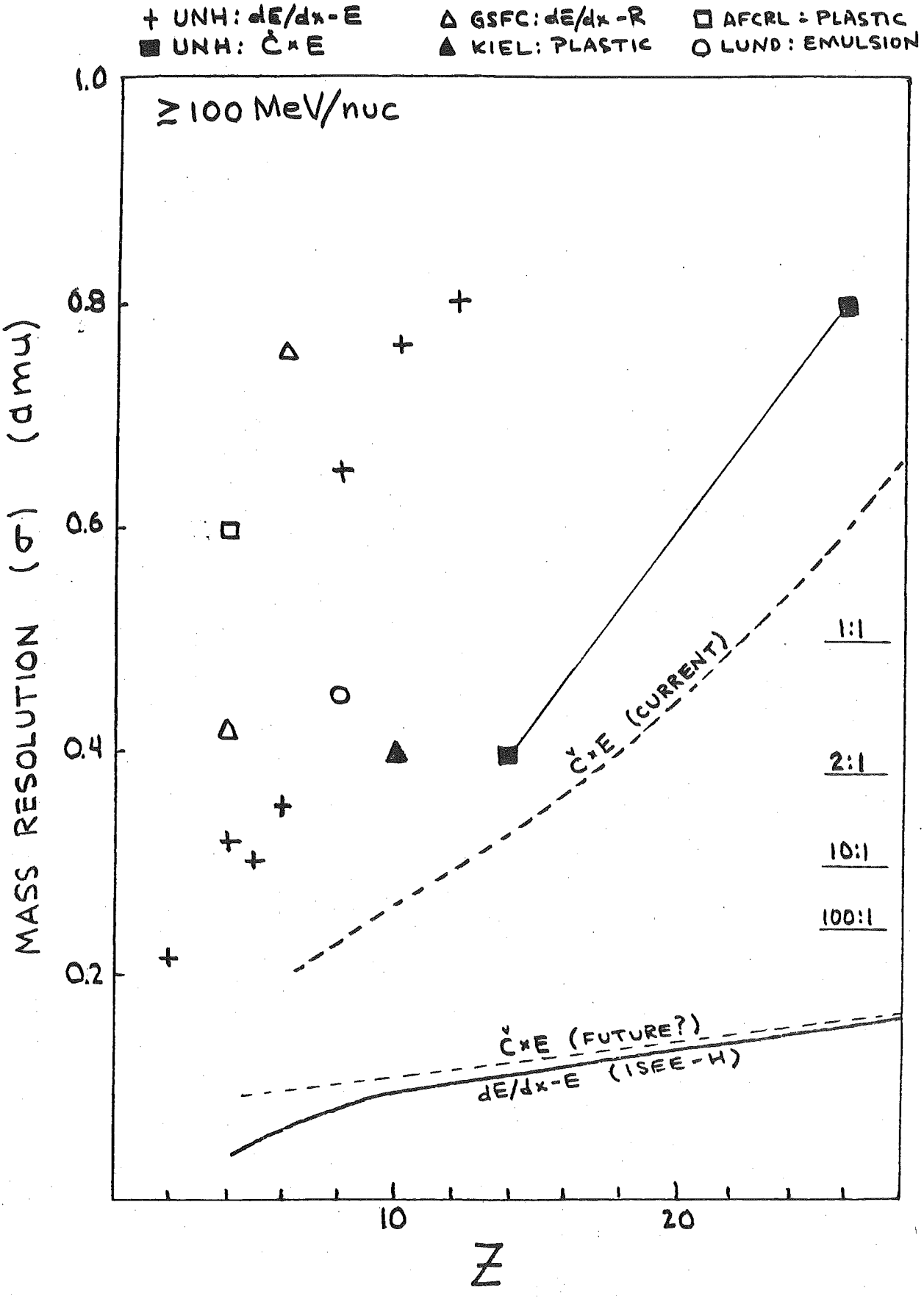
+ UNH: dE/dx-E
■ UNH: Č×E
△ GSFC: dE/dx-R
▲ KIEL: PLASTIC
□ AFCRL : PLASTIC
○ LUND : EMULSION
≥100 MeV/nuc
MASS RESOLUTION (σ) (amu)
1.0
0.8
0.6
0.4
0.2
10
20
Z
Č×E (CURRENT)
Č×E (FUTURE?)
dE/dx-E (ISEE-H)
1:1
2:1
10:1
100:1

Fig. 6

TYPICAL FUTURE SATELLITE $dE/dX - E$ TELESCOPES

MISSION	GROUP	ΔE	E^1	$A\Omega$ (CM^2 SR)	RANGE (MEV/ NUC)
HELIOS (75)	GSFC	DISK	SI	~0.2	~6 - 200
MJS (77)	CIT/GSFC/UNH	CURVED	SI	~6	~2 - 120
ISEE (M) (77)	CHICAGO	CURVED	CsI	~2	
ISEE (H) (78)	GSFC	CURVED	SI	~2	~8 - 120
	CIT	POSITION	SI	~1	~2 - 200
	LBL	POSITION	SI	~10	~40 - 500

Fig. 7

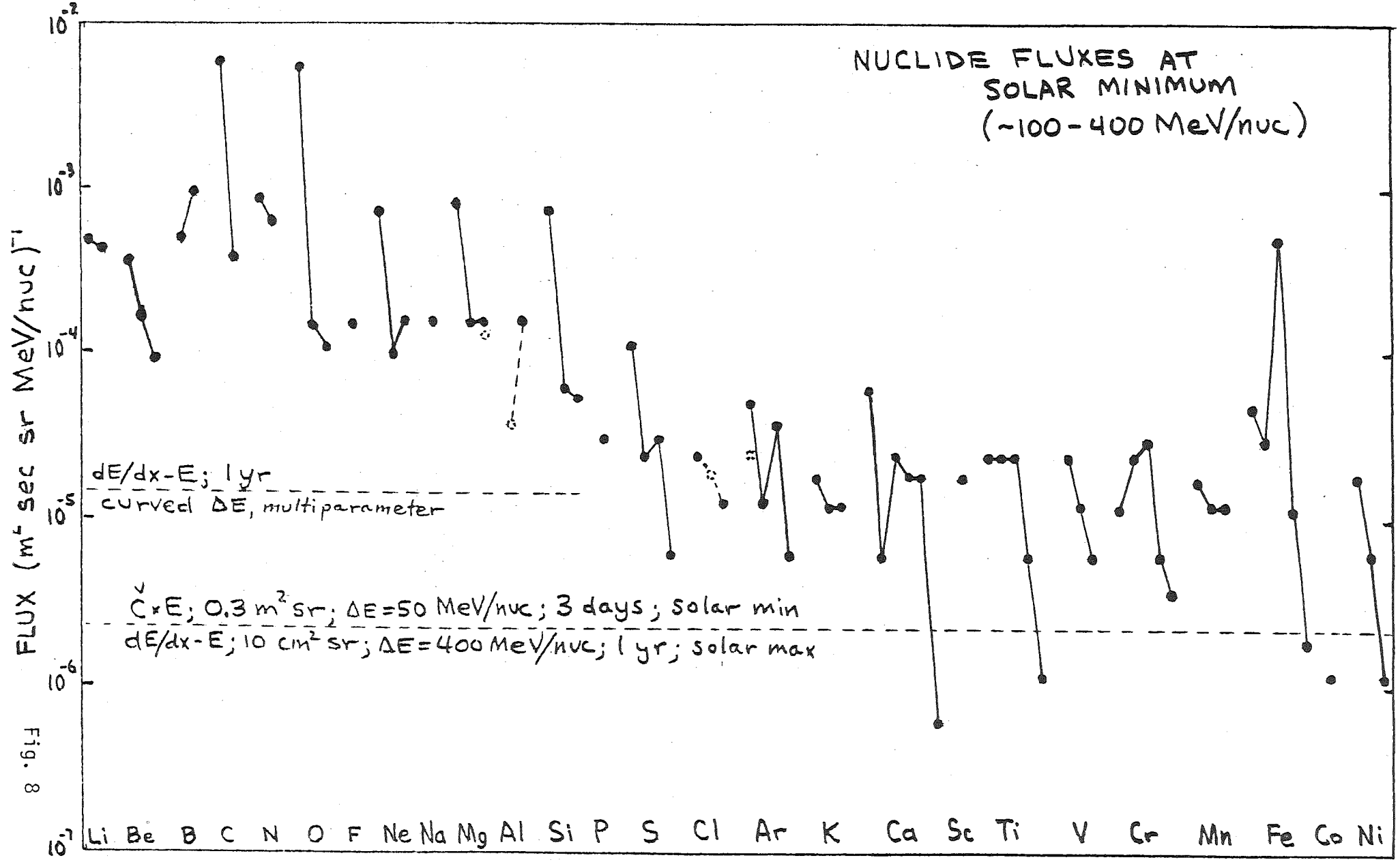
NUCLIDE FLUXES AT
SOLAR MINIMUM
(~100-400 MeV/nuc)
FLUX (m² sec sr MeV/nuc)⁻¹
10⁻²
10⁻³
10⁻⁴
10⁻⁵
10⁻⁶
10⁻⁷
dE/dx-E; 1 yr
curved ΔE, multiparameter
C̆ x E; 0.3 m² sr; ΔE=50 MeV/nuc; 3 days; solar min
dE/dx-E; 10 cm² sr; ΔE=400 MeV/nuc; 1 yr; solar max
Li Be B C N O F Ne Na Mg Al Si P S Cl Ar K Ca Sc Ti V Cr Mn Fe Co Ni

Fig. 8

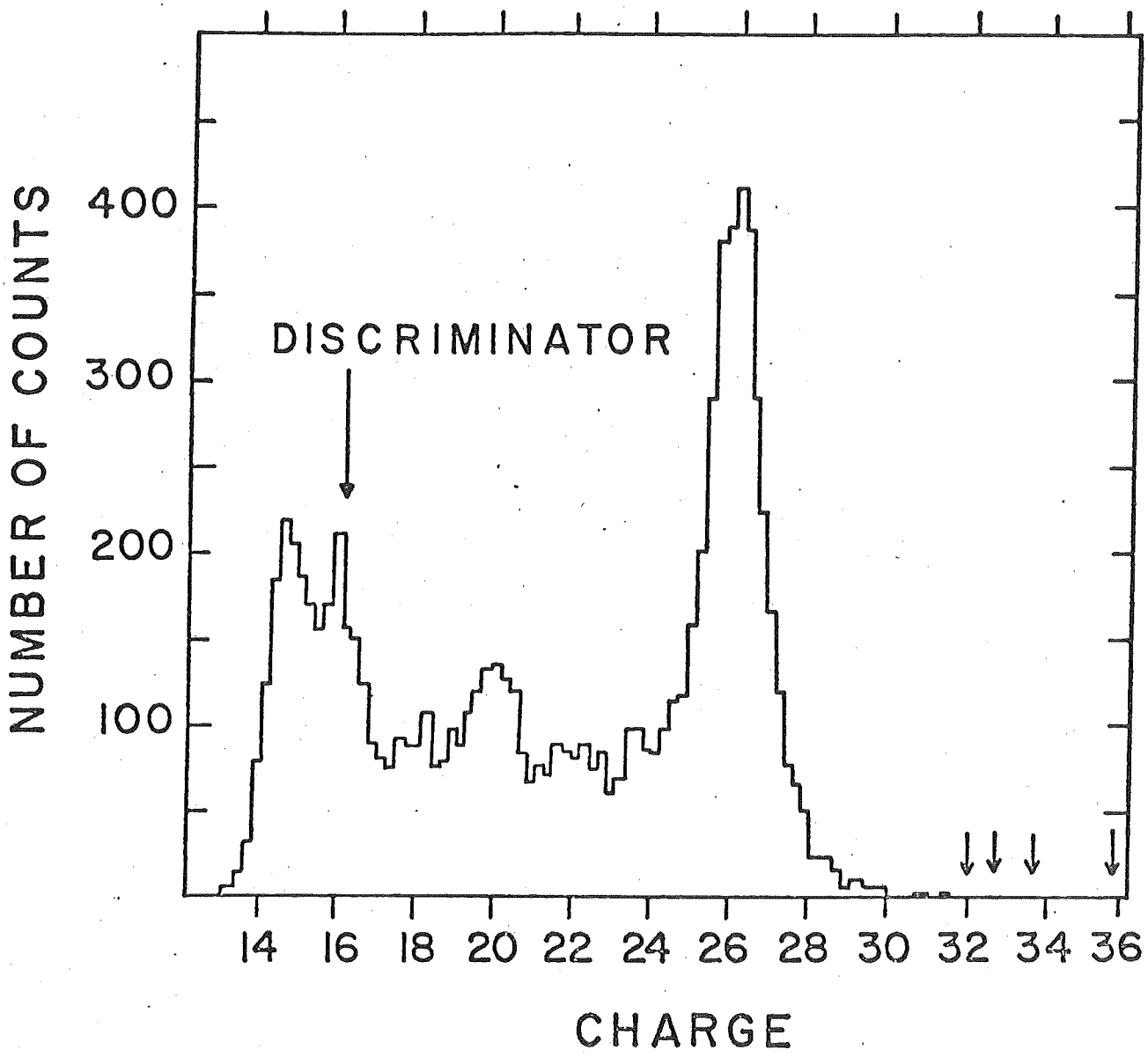
NUMBER OF COUNTS
400
300
200
100
DISCRIMINATOR
14
16
18
20
22
24
26
28
30
32
34
36
CHARGE

Fig. 9

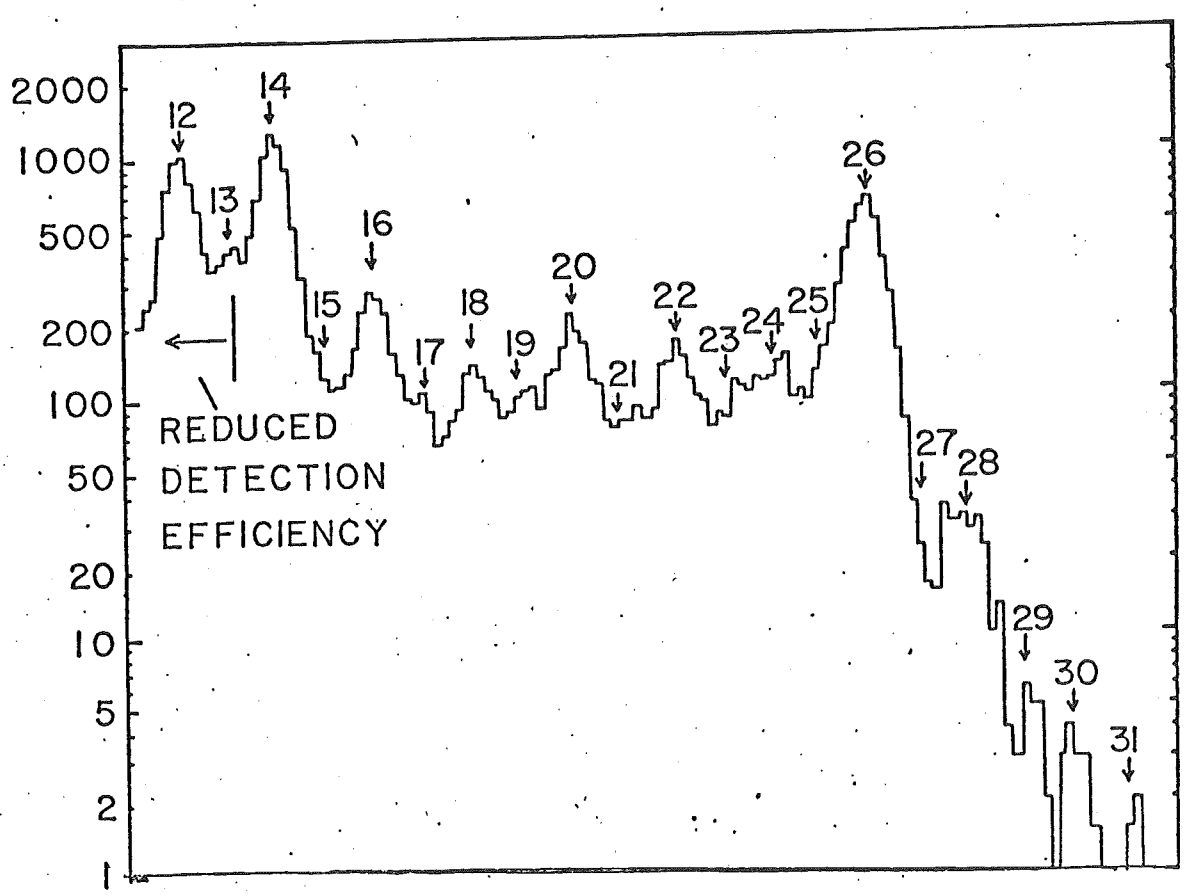
2000
1000
500
200
100
50
20
10
5
2
1
12
13
14
15
16
17
18
19
20
21
22
23
24
25
26
27
28
29
30
31
REDUCED
DETECTION
EFFICIENCY

Fig. 10

ELEMENTAL RESOLUTION

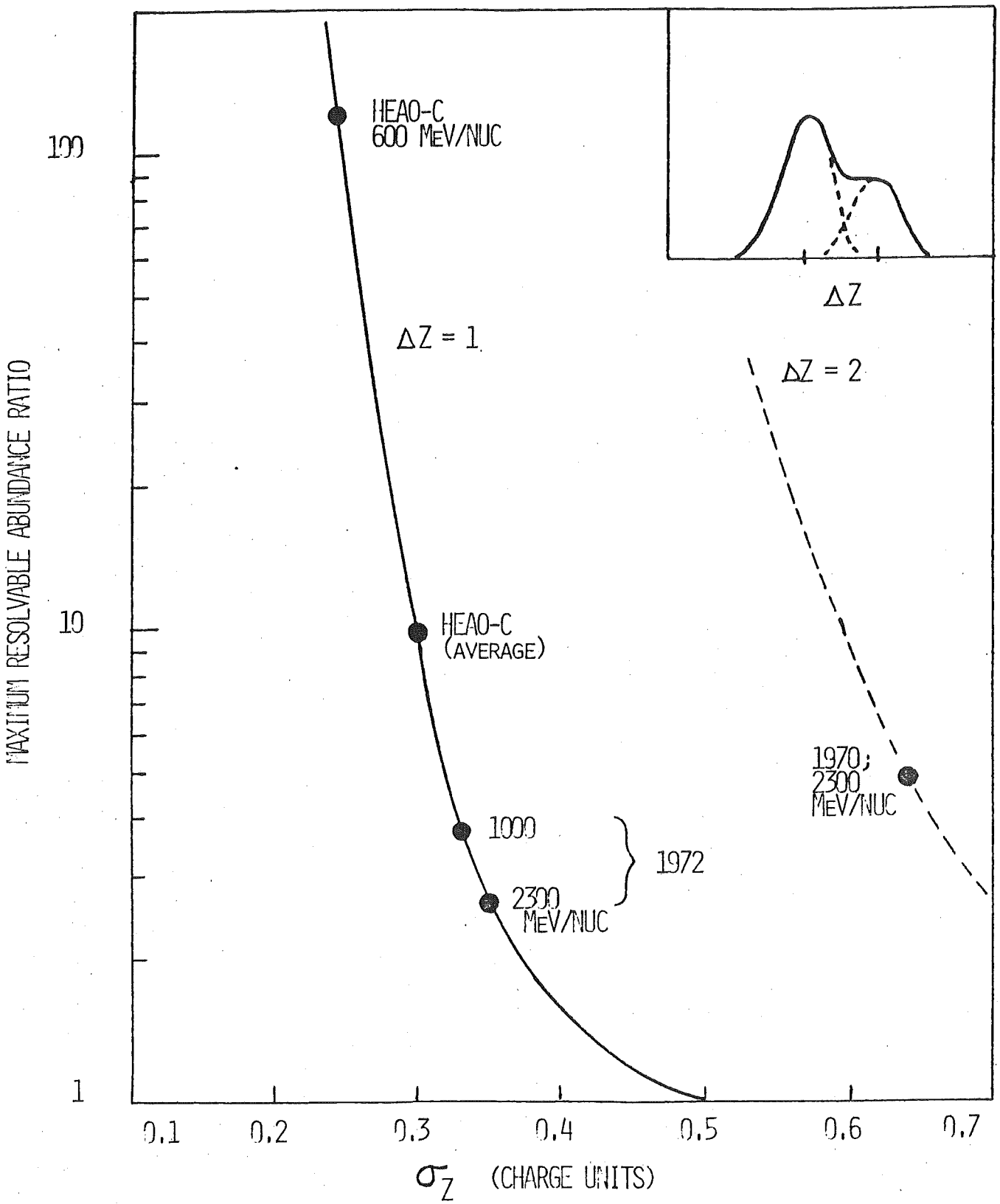

Fig. 11

UH COSMIC RAYS

PLANNED SATELLITE EXPERIMENTS

MISSION	GROUP	CHARGE RESOLUTION	$A\Omega$ M^2SR	TECHNIQUE
UK6	BRISTOL	~0.3 (Fe)	2	SPHERICAL
1977		~0.8 (Pb)		$dE/dX - \check{C}$
HEAO-C	CIT/MDRL/	~0.30 (Fe)	4	PLANAR
1979	UM/WU	~0.36 (Pb)		$dE/dX - \check{C}$
				HODOSCOPE

Fig. 12

HEAO-C: EVENTS/YR

$35 \leq Z \leq 50$	~3000
$Z > 50$	~1000
$Z \geq 80$	~ 150